ARTICLE

OBC
www.rsc.org/obc

Expected and unexpected results from combined β-hairpin design elements †

Muthu Dhanasekaran,[a,c] Om Prakash,[b] Yu Xi Gong[b] and Paul W. Baures*[a,d]

[a] *Department of Chemistry, 111 Willard Hall, Kansas State University, Manhattan, KS, USA*
[b] *Department of Biochemistry, 103 Willard Hall, Kansas State University, Manhattan, KS, USA*
[c] *Department of Chemistry, University of Arizona, Tucson, AZ, USA*
[d] *Department of Chemistry, 6600 College Station, Bowdoin College, Brunswick, ME, USA. E-mail: pbaures@bowdoin.edu; Fax: 207-725-3017; Tel: 207-725-3637*

Received (in Pittsburgh, PA, USA) 24th November 2003, Accepted 9th June 2004
First published as an Advance Article on the web 24th June 2004

A model β-hairpin dodecapeptide [EFGWVpGKWTIK] was designed by including a favorable D-ProGly Type II′ β-turn sequence and a Trp–zip interaction, while also incorporating a β-strand unfavorable glycine residue in the N-terminal strand. This peptide is highly folded and monomeric in aqueous solution as determined by combined analysis with circular dichroism and ^{1}H NMR spectroscopy. A peptide representing the folded conformation of the model β-hairpin [cyclic(EFGWVpGKWTIKpG)] and a linear peptide representing the unfolded conformation [EFGWVPGKWTIK] yield unexpected relative deviations between the CD and ^{1}H NMR spectroscopic results that are attributed to variations in the packing interactions of the aromatic side chains. Mutational analysis of the model β-hairpin indicates that the Trp–zip interaction favors folding and stability relative to an alternate hydrophobic cluster between Trp and Tyr residues [EFGYVpGKWTIK]. The significance of select diagonal interactions in the model β-hairpin was tested by rearranging the cross-strand hydrophobic interactions to provide a folded peptide [EWFGIpGKTYWK] displaying evidence of an unusual backbone conformation at the hydrophobic cluster. This unusual conformation does not appear to be a result of the glycine residue in the β-strand, as replacement with a serine results in a peptide [EWFSIpGKTYWK] with a similar and seemingly characteristic CD spectrum. However, an alternate arrangement of hydrophobic residues with a Trp–zip interaction in a similar position to the parent β-hairpin [EGFWVpGKWITK] results in a folded β-hairpin conformation. The differences between side chain packing of these peptides precludes meaningful thermodynamic analysis and illustrates the caution necessary when interpreting β-hairpin folding thermodynamics that are driven, at least in part, by aromatic cross strand interactions.

Introduction

β-Hairpins as β-sheet models

The identification of monomeric and water-soluble β-hairpins has enabled their analysis and thus contributed to a better understanding of the factors that direct the formation of stable protein β-sheet structure.[1–9] Likewise, artificial β-sheet nucleators have also been valuable in studying parallel and antiparallel β-sheet structure.[10–14] The following sections briefly introduce the factors that have been studied in the context of β-hairpin and β-sheet structure.

Intrinsic φ, ψ propensities

The preference of an amino acid residue to adopt a particular form of secondary structure in lieu of another has been used to help explain and predict the formation of β-hairpins, although the context dependency of the amino acid is also known to influence the ϕ, ψ propensities.[9,15–17] Glycine within a β-strand is destabilizing relative to other amino acids, although simultaneous introduction of cross-strand aromatic interactions have been shown to be capable of "rescuing" β-sheet formation when glycine is present.[18]

β-Turn or loop residues

The nature of the residues between the two β-strands on antiparallel β-hairpin formation and stability has been examined and it is now common to incorporate D-ProGly as the $i + 1$ and $i + 2$ residues of a type II′ β-turn in many designed β-hairpins.[19–25] There are, however, alternative ways to form a turn in a β-hairpin and this is important in the β-hairpin classification.[26,27]

Side chain interactions

The role of the side chains in β-hairpin formation and stability has been the subject of several studies, including those that examined context dependency,[28,29] electrostatic interactions,[30,31] cross-strand interactions,[32,33] lateral and diagonal pairings,[34–36] and positional dependency of the side chains.[17,37] The cross-strand pairing of Trp side chains in β-hairpin formation is a significant stabilizing interaction.[38] A similar pairing between Trp residues was part of a cyclic peptide mimic of an antibody hypervariable loop.[39]

Length

The length of a β-hairpin has been shown to influence stability.[40]

Cooperativity

The ability of a β-hairpin to show cooperative folding has been explored and is important to the validity of the two-state models used for thermodynamic analysis.[41–43] Three-stranded β-sheets are also useful for exploring cooperativity in sheet formation.[44–47]

Aggregation

Early β-sheet models suffered from aggregation, whereas many designed β-hairpins have now been shown to be monomeric

† Electronic supplementary information (ESI) available: Circular dichroism spectra, ^{1}H NMR NOE figures, molecular dynamic results. See http://www.rsc.org/suppdata/ob/b3/b315228f/

DOI: 10.1039/b315228f

in aqueous solution.[1–9] The presence of like charges within a β-hairpin has been proposed to decrease the aggregation tendency, although aggregation has even been observed for highly charged peptides.[44]

Methodology for studying β-hairpin solution structure

Circular dichroism, 2D-^{1}H NMR spectroscopy, and analytical ultracentrifugation have been the most important tools in analyzing β-hairpins in solution[1–9] and in studying the thermodynamics of β-hairpin folding and stability.[19–25,30–38,40–51] The interpretation of NMR data has been the focus of several reports.[52–57]

Molecular modeling is often used in the analysis of ^{1}H NMR data collected on β-hairpins; however, simulations of folding have also been useful in the analysis of β-hairpin structure.[58–70]

Design, purpose and mutational analysis of a model β-hairpin

Our goal at the outset of this work was to identify a model β-hairpin that could serve as the starting point for peptidomimetic incorporation within one of the two β-strands for the purpose of determining the thermodynamic consequences in terms of folding. We reasoned that such thermodynamic consequences would be valuable information for appropriate use of existing peptidomimetics[71–75] as well as in the design of new β-strand peptidomimetics.

We chose a peptide dodecamer for our starting point, as this is of sufficient length to yield a stable β-hairpin.[38] The D-Pro-Gly sequence yields a β-turn that serves as β-hairpin nucleator[56] and therefore favors β-hairpin formation.[19–25] In addition, the β-branched Val introduced prior to the D-Pro residue enforces the *trans*-amide isomer at D-Pro.[76,77] This peptide and the others studied in this paper are shown in Fig. 1. The design of the parent β-hairpin, **1**, also includes a Trp–zip interaction.[38] This was included in anticipation that the Trp–zip interaction would maintain a similar fold between peptides and favor folding even when unfavorable amino acids for β-strand formation were included in the sequence. A glycine was included in one β-strand in order to create a position for subsequent introduction of biologically-significant β-strand peptidomimetics.[71–75] The folding and comparative analysis of **1** was determined by replacing D-Pro in the β-turn with L-Pro in order to yield an unfolded peptide model, **2**, and by preparing a cyclic peptide, **3**, as a folded model for comparison by both CD and NMR spectroscopy.[78] Peptide **4** tests the significance of the Trp–zip interaction in **1**. We also designed **5**, a peptide with a β-strand glycine in a non-hydrogen bonding location with respect to **1**. The change to **5** from **1** alters the location of the Trp–zip as well as the cross strand interactions, but was done to yield a model β-hairpin for peptidomimetic incorporation in a non-hydrogen bonded location for comparison with the hydrogen bonded location in **1**. Peptide **5** adopts an β-hairpin solution structure with an unusual backbone conformation. Peptide **6** examines the role of the β-strand Gly in the formation of this unusual conformation while **7** attempted to create a similar conformation within a different β-hairpin context.

```
1     EFGWVpGKWTIK
2     EFGWVPGKWTIK
3    (EFGWVpGKWTIKpG)
4     EFGYVpGKWTIK
5     EWFGIpGKTYWK
6     EWFSIpGKTYWK
7     EGFWVpGKWITK
```

Fig. 1 Peptide sequences.

Experimental

Peptide synthesis and purification

Peptides **1**–**7** were synthesized by standard solid-phase procedures based on fluorenylmethoxycarbonyl (Fmoc) chemistry. Wang resins preloaded with the C-terminal amino acid were purchased along with commercially available pentafluorophenyl ester activated amino acids that were used for most coupling steps (Advanced Chemtech). Preactivation of the Fmoc-amino acid with HBTU was used for some amino acids not readily available in the preactivated form. Amino acids with potentially reactive side chains, most importantly the Trp residues, were incorporated with the side chains (Boc) protected. Each coupling was performed manually in DMF (dimethylformamide) with the resin suspended by bubbling N_2. Following the coupling, the DMF was drained and the resin was rinsed five times with DMF. A Kaiser test was performed on the resin to determine if free amines remained. If so, the coupling was repeated until the Kaiser test was negative by visual inspection of the beads. The Fmoc group was deprotected with a solution of 20% piperidine in DMF and was followed by another rinsing of the beads. The peptides were cleaved from the resin by using the cleavage cocktail trifluoroacetic acid–water–triethylsilane (90 : 5 : 5) for 90 min. Post-cleavage workup involved removal of the trifluoroacetic acid under vacuum followed by precipitation of the peptide with ether. In addition, **3** was synthesised by the methodology that has been described previously.[79] Briefly, we anchored the side-chain of Fmoc-Glu-OAll to the Wang resin before using Fmoc-based peptide synthesis to complete the entire length of the peptide. The allyl protecting group was then removed by using $Pd(PPh_3)_4$ in $CHCl_3$–AcOH–*N*-methylmorpholine (37 : 2 :1) for 3 h. This deprotection step was followed by head-to-tail cyclization in the presence of HBTU before final cleavage from the resin. In each case the peptide was dissolved in water, lyophilized, and then purified by preparative RP(C18)-HPLC in an acetonitrile–water gradient containing 0.1% TFA. Homogeneity of the final peptide was assured by analytical RP-HPLC and MALDI mass spectrometry.[80]

Circular dichroism

All of the circular dichroism experiments were carried out on JASCO 810 spectropolarimeter at 293 K. The spectra were recorded from 180 to 250 nm by using the continuous mode with a 1 nm bandwidth, a 4 s response, and a scan speed of 100 nm min^{-1} in cells with a path length of 0.2 cm. Five scans were accumulated and averaged for each spectrum. The instrument was calibrated by using d^{10}-camphorsulfonic acid. Peptide stock solutions were prepared by weighing the required amount to make 1 mL of a 1.5 mM solution and the pH was adjusted to the desired value. Samples were prepared by diluting the stock solution to 150 μM.

^{1}H NMR Spectroscopy

All NMR spectra were recorded on a Varian UNITYplus 500 MHz spectrometer. Peptide concentrations for the NMR experiments varied from 2 to 3 mM. Samples were dissolved in 0.7 mL of H_2O–D_2O (9 : 1 ratio by volume) or in 0.7 mL D_2O depending on the experimental requirement. The invariant nature of NMR chemical shifts and line widths upon ten-fold dilution indicates that peptides **1**–**5** and **7** are monomeric in aqueous solution at the concentration used for 2D-NMR analysis. The pH of each sample was adjusted to 5.0 by using DCl or NaOD as necessary. All of the 2D-NMR experiments were performed at 283 K. The amino acid spin system was identified by using TOCSY. The sequential assignment was made by the combined use of TOCSY and NOESY spectra. The spectra were recorded by standard techniques using presaturation of the water and the time proportional phase increment method (TPPI). Mixing times of 200, 300 and 400 ms were used for NOESY experiments. A mixing time of 100 ms was used for the TOCSY experiments. A shifted square sine bell window function was used in both dimensions. A mixing time of 200 ms was used for distance constraints measurements.

Coupling constants ($^3J_{\alpha H-NH}$) were measured directly from 1D spectra or by using 2D DQF-COSY spectra.

Molecular modeling

Molecular dynamics simulation was done with the INSIGHT/DISCOVER package (Molecular Simulations, Inc., San Diego, CA). The starting structure had extended conformation ($\phi = -180°$ and $\psi = 180°$) for the strand residues, whereas the D-Pro–Gly segment was an ideal type II′ ($\phi_{i+1} = 60°$ and $\psi_{i+1} = -120°$, $\phi_{i+2} = -80°$ and $\psi_{i+2} = 0°$) β-turn. A distance dependent dielectric constant (2.5r where r is the distance in Å) was used. All peptide bonds were constrained to trans conformations by a 100 kcal rad^{-1} energetic penalty. Distance restraints with a force constant of 25 kcal mol^{-1} were applied in the form of a flat-bottom potential well with a common lower bound of 2.0 Å and an upper bound of 3.0, 4.0 and 5.0 Å, respectively, in accordance with observed strong, moderate or weak NOE intensities. No dihedral angle or hydrogen bond constraints were employed. NOE signals that overlap were not included in the restraint file. The starting structure was minimized with all restraints in place, first with steepest descent and then with conjugate gradient algorithm, and finally subjected to simulated annealing. A two hundred picosecond molecular dynamics run was done at 1000 K, followed by cooling to 300 K in 7 steps for a total of 35 ps, and then steepest descent and conjugate gradient minimization. 100 final minimized structures were sampled at 2 ps intervals.

Results

The design of the parent peptide, **1**, incorporates several features known to be relevant to the formation of stable, monomeric β-hairpin structure in water: namely, the presence of a D-ProGly type II′ β-turn,[18] cross-strand Trp residues,[16,24] and charged residues that aid water solubility and create overall charge to prevent aggregation.[1–9] Peptide **1** is an appropriate length to favor stability[39] and also locates the hydrophobic groups nearby the β-turn.[34]

Circular dichroism (CD) spectroscopy is a powerful tool for identifying secondary structure in both peptides and proteins.[81–84] Yet, many short designed β-hairpin peptides have shown no characteristic β-sheet CD signals even though they are well defined β-hairpins when characterized by NMR spectroscopy.[48,85] Indeed, proteins rich in β-sheet can be classified by their CD signal leading to one class of structures that appears folded by CD and another class that appears unfolded by CD.[86]

The CD spectrum of **1**, Fig. 2, has a strong exciton coupling signal[87,88] resulting from the W4–W9 cross-strand pair that overwhelms the anticipated signal characteristic of β-sheet structure (215–218 nm single minima). The CD signal at 215 nm changes moderately upon addition of MeOH (19% of the molar ellipticity value observed in 50% MeOH), whereas the spectrum changes only slightly at 227 nm (5% of the molar ellipticity value observed in 50% MeOH). Methanol has previously been used to help promote β-hairpin formation.[48] In this case, the addition of methanol only slightly increases the CD signal and suggests that the peptide undergoes little change in folding with MeOH addition. The percentage of folded peptide without added MeOH is not significantly affected by influence of pH as shown in the inset for Fig. 2.

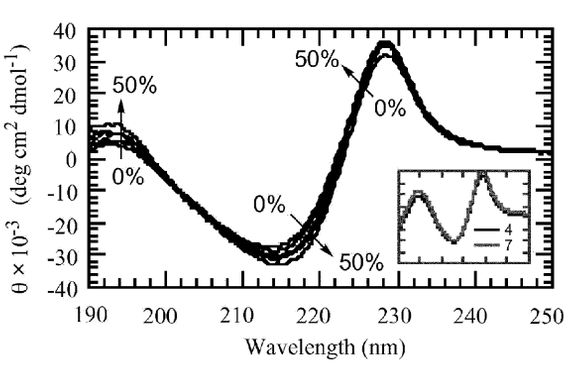

Fig. 2 The CD spectra of **1** recorded as a function of increasing MeOH concentration. The inset figure compares the CD spectrum at pH 4 and 7 in water. The axes on the inset graph are identical to the large graph.

Peptide **2** substitutes a D-Pro residue in the type II′ β-turn with L-Pro, thereby created an unfolded peptide model for comparison. Similarly, **3** incorporates a second D-ProGly turn to force cyclization and serve as a model folded structure. To understand the importance of the Trp–zip interaction in the folding of **1**, a Tyr-containing mutant, **4**, was prepared and characterized. The CD spectra for **1**–**4** recorded in water are compared in Fig. 3.

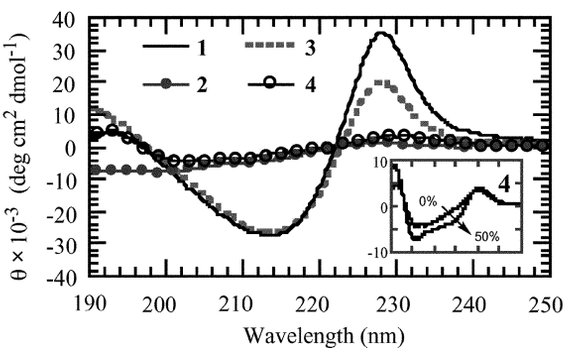

Fig. 3 The CD spectra of **1**–**4** recorded in water. The inset figure compares the CD spectra of **4** recorded as a function of MeOH concentration. The *x*-axis on the inset graph is identical to the large graph.

As anticipated, a random coil signal for **2** was observed, while **3** yields a signal similar to **1**. The fact that the signal at 227 nm is significantly less intense for **3** as compared with **1** while the signal at 215 nm is of like intensity between the two peptides was unanticipated. The Trp–zip interaction for **1** was modified with a W4Y substitution to yield **4**, thereby disrupting the W4–W9 cross-strand pair and resulting in the expected loss of the 227 nm signal (Fig. 2).[12] Peptide **4** has a negligible CD signal at 215 nm as compared with **1**—largely due to loss of the exciton signal, as the positive CD signal below 200 nm is suggestive of a partially-folded structure. It is not possible to know the exact ratios of peptide backbone conformation *vs.* side chain interactions that contribute to the signal at 215 nm in order to compare the CD spectra of **1** with **4**. We note that addition of MeOH to **4** influences the signal at 215 nm (an increase of 58% of the molar ellipticity value observed in 50% MeOH) as well as the signal at 195 nm (an increase of 16% of the molar ellipticity value observed in 50% MeOH) significantly more than the signal at 227 nm (a *decrease* of 6% of the molar ellipticity value observed in water) (Fig. 3 inset). The relative intensities in the CD spectra of **1** upon MeOH addition also changed more at 215 nm than at 227 nm.

Peptides **1** and **4** have well dispersed NH and $C_\alpha H$ ^{1}H NMR chemical shifts indicative of a folded structure. These chemical shifts are concentration independent below 3 mM and provide NOE cross-peaks consistent with antiparallel β-hairpin formation—supporting both the expected hydrogen bonding register and the presence of the β-turn. The chemical shift assignments for **1**–**4** are given in Table 1 except for the assignments for the aromatic ring hydrogens that are given in Table 2. Also included in Table 1 are the $C_\alpha H$ chemical shift deviations from published random coil values.[89]

The TOCSY spectra for **1** and the residue assignments, plus selected NOESY spectra, are available in the supporting

Table 1 Chemical shifts (ppm), coupling constants, and chemical shift deviations (ppm) for **1**–**4**[a]

	Residue	NH	$C_\alpha H$	$^3J_{\alpha NH}$/Hz	$C_\beta H$	$C_\gamma H$	$C_\delta H$	$C_\varepsilon H$	NH_3^+	$\Delta\delta C_\alpha H$	$\Delta\delta NH$
1:	Glu1		3.98		2.05, 2.30					−0.31	
2:			3.94							−0.35	
3:		7.71	4.62	9.5	1.92	2.05, 2.19				0.33	−1.12
4:			3.99		2.04	2.30				−0.30	
	Phe2	8.81	4.72	8.5	1.74, 2.55					0.10	0.20
		8.93	4.56							−0.06	0.32
		8.36	4.66	8.5	1.81, 2.49					0.04	−0.25
		8.86	4.82		2.53, 2.83					0.20	0.25
	Gly3	8.31	3.37, 3.51							−0.50	−0.35
		8.46	3.85							−0.16	−0.20
		8.01	3.42, 3.58	Overlap						−0.43	−0.65
		8.33	3.52, 3.63							−0.38	−0.33
	Trp4	8.49	5.08	7.5	3.11, 3.35					0.41	0.03
		8.06	4.54							−0.13	−0.40
		8.59	4.93	7.0	3.08, 3.34					0.26	0.13
	Tyr4	8.48	4.88	8.0	2.53, 2.83					0.32	−0.11
	Val5	9.40	4.64	9.5	2.03	0.82, 0.97				0.51	0.89
		7.72	4.20							0.07	−0.79
		9.29	4.65	9.0	2.07	0.84, 0.95				0.52	0.78
		8.88	4.53		1.98	0.82, 0.94				0.40	0.37
	D-Pro6		4.40		2.00	2.40	3.85, 3.93			−0.04	
	L-Pro6		4.00							−0.44	
			4.41		2.08, 2.11	2.20, 2.43	3.86, 3.95			−0.03	
			4.38		1.94, 2.38	2.10	3.84			−0.06	
	Gly7	8.72	3.85, 4.08							0.07	0.06
		8.31	3.77							−0.04	−0.35
		8.73	3.85, 4.08	Overlap						−0.07	0.07
		8.38	3.69, 4.03							0.02	−0.28
	Lys8	8.09	4.92	10	1.89	1.50	1.78	3.06	7.64	0.60	−0.58
		8.01	4.19							−0.13	−0.66
		8.13	4.34	9.5	1.89	1.41, 1.47	1.78		3.07	0.02	−0.54
		7.87	4.74	9.5	1.88	1.41	1.71, 1.79	3.02		0.42	−0.80
	Trp9	8.89	4.42	6.5	2.03, 2.92					−0.25	0.43
		8.19	4.78							0.11	−0.27
		9.09	4.34	6.0	2.10, 2.93					−0.33	0.49
		8.99	4.58	6.0	2.91, 3.19					−0.09	0.53
	Thr10	8.63	4.55	8.5	3.93	1.12				0.16	0.11
		8.01	4.29							−0.10	−0.57
		8.72	4.50	Overlap	4.08	1.12				0.11	0.20
		8.65	4.53	8.0	3.99	1.12				0.14	0.13
	Ile11	7.73	3.63	7.0	1.46	1.13, 1.46	0.70			−0.55	−0.79
		8.16	4.10							−0.08	−0.36
		8.04	3.61	Overlap	1.30	Overlap	0.58, 0.66			−0.57	−0.48
		7.91	3.86	7.0	1.58	1.35, 1.35	0.76			−0.32	−0.61
	Lys12	8.01	3.98	7.5	1.59	1.17	1.46	2.84	7.58	−0.34	−0.66
		8.00	4.14							−0.18	−0.67
		8.40	4.60	9.0	1.56	1.24, 1.29	1.44	2.85		0.28	−0.27
		8.01	4.06	7.5	1.64	1.19	1.48	2.82		−0.26	−0.66
3:	D-Pro13		4.33		1.96	2.13, 2.23	3.50, 3.66			−0.11	
3:	Gly14	8.56	3.74, 3.98							−0.15	−0.10

[a] Peptides **1**–**4** are organized as lines 1–4, respectively, for any given row in this table. Amino acid mutations in **2** and **4** are specifically indicated under the residue column. Random coil values were taken from ref. 89.

information.† The $^3J_{\alpha H-NH}$ couplings for **1** are largely consistent with β-strand formation. In addition, both the G3 and G7 geminal $C_\alpha H$ proton signals are split (125 Hz), indicating that the protons are in a rigid conformation and supportive of a folded structure. The NOEs observed support the conclusion that the peptide is folded in water, but possibly with splayed ends since contacts between N- and C-terminal residues were not observed. Thus, 3G–T10 and 5V–8K $d_{(NN)}$ NOE cross peaks as well as the W4–W9 $d_{(\alpha\alpha)}$ NOE cross peak indicate the formation of a hairpin structure about a β-turn whose formation was supported by the observed 5V–8K and 7G–8K $d_{(NN)}$ cross peaks.

Additional support for the folding of **1** into a β-hairpin structure comes from analysis of the NOE spectrum in which there are signals between cross-strand residue pairs F2–I11 and W4–W9, NOEs that also clearly support the formation of a hydrophobic cluster. The Ile δ-CH_3 upfield shift over its random coil value is 0.2 ppm[89] and is evidence that this residue is

Table 2 Chemical shifts (ppm) for the aromatic ring hydrogens in **1**, **3** and **4**

		Ring hydrogen						
	Residue	1	2	3	4	5	6	7
1:	Phe2		6.77	7.28	6.67	7.28	6.77	
3:			6.75	7.14	7.25	7.14	6.75	
4:			6.98	7.34	7.23	7.34	6.98	
	Trp4	10.28	7.48		7.18	7.30	6.77	7.28
		10.32	7.48		7.20	7.30	7.02	6.54
	Tyr4		6.86	6.82		6.82	6.86	
	Trp9	9.65	6.77		5.38	6.61	7.08	7.17
		9.62	6.80		5.28	7.02	7.14	7.18
		9.82	7.01		7.23	6.35	6.92	7.13

Peptides **1**, **3** and **4** are organized as lines 1–3, respectively, for any given row in this table. Amino acid mutations in **4** are specifically indicated under the residue column.

involved in the hydrophobic cluster. Moreover, a diagonal interaction between side chains is apparent by the observed NOE signal between F2 and W9. The strong NOE between W4 and W9 and the strong/moderate NOEs between F2 and W9 were significant in providing constraints for the molecular dynamic determination of the geometry of the two Trp rings relative to one another and to the backbone of the β-hairpin.

Peptide **2** serves as an unfolded model and CD analysis supported the formation of a random coil conformation (Fig. 3). Regardless, 2D NMR experiments were undertaken in order to search for evidence of long-range contacts that might provide evidence of a folded structure. This effort failed immediately due to the significant overlap of the chemical shifts for the different residues. Such a lack of chemical shift dispersity is consistent with a random coil conformation. In contrast, the cyclic folded model, **3**, was easily characterized for comparative purposes because the chemical shifts were widely dispersed, much like those observed for **1**, and with signals largely downfield from random coil values for the strand residues (Table 1). The NOESY spectrum for **3** contains the $d_{(NN)}$ NOE cross peaks 1E–14G, 3G–10T, 5V–8K and 7G–8K, consistent with a β-hairpin and two type II′ β-turns. Surprisingly, the expected E1–K12 $d_{(NN)}$ NOE was not observed.

Selected NOEs for **3** are different as compared to **1**. For example, the side chain F2:βH–W9:7H cross peak observed for **1** is not present in **3**, whereas both a weak $C_\alpha H$–$C_\alpha H$ NOE between F2 and I11 and a strong side chain 2F:4H–I11δH NOE is observed in **3** even though they were not present in **1**.[90] These differences suggest that the cyclic constraint in **3** results in cross strand interactions to form even when diagonal interactions were favored in **1**.

Peptide **4** does not have a Trp–zip interaction but does retain the potential for hydrophobic cluster formation. The CD spectrum of **4** is visibly different because the strong exciton coupling of the two Trp rings in **1** is absent in **4**. The ^{1}H NMR analysis of **4** supports the formation of a partially folded conformation in water. Interestingly, **4** seemingly adopts a conformation similar to **3** wherein only the cross strand side chains interact, as no NOEs for diagonal interactions were observed. Instead, NOEs are observed between I11:δH and I11:γH with the 2F:3,5H as well as I11:αH with 2F:6H. Likewise, a cross strand NOE peak between 4Y:3,5H and 9W:βH is observed. It is important to note that the only backbone interstrand cross peak apparent for **4** is the Y4–W9 $d_{(\alpha\alpha)}$ NOE and that even this cross peak is ambiguous given its proximity to the water signal.

A graphical NOE summary for **1**, **3** and **4** is available in the supporting information. † The different NOEs observed between peptides **1**, **3** and **4** indicate that these model β-hairpins adopt different relative folded conformations that preclude meaningful thermodynamic analysis. Moreover, the observed differences between **1** and the cyclic folded model peptide, **3**, indicates that the method of quantification of folding thermodynamics must be chosen with care.

The peptides **1** and **3** appear significantly folded by both CD and NMR analysis with the possible caveat as described previously for the N- and C-terminal residues of **1**. It is also evident that **4** either adopts a partially folded structure or is more conformationally dynamic, or both. Yet the observed chemical shift deviations from the structured peptides with those values associated with random coil structure—a method often used as a general indicator of peptide structure and conformation[89,91] —fail to add support for this conclusion. Indeed, the observed chemical shifts do not result in a general downfield deviation expected for β-strand residues and also vary between the peptides for particular residue positions (Fig. 4). Peptide **2** was prepared as an unfolded model system, although this peptide also shows chemical shift deviations with respect to known random coil values.[89] Comparison of the chemical shift deviations for **1**, **3** and **4** with that of **2** yields results that are still inconsistent with the expectation of downfield shifts for the β-strand $C_\alpha H$ protons. We think that at least one factor contributing to this anomaly is the presence of the aromatic rings proximal to the C_α protons, an effect described previously in β-hairpins and L-Pro unfolded model peptides.[37,40,92]

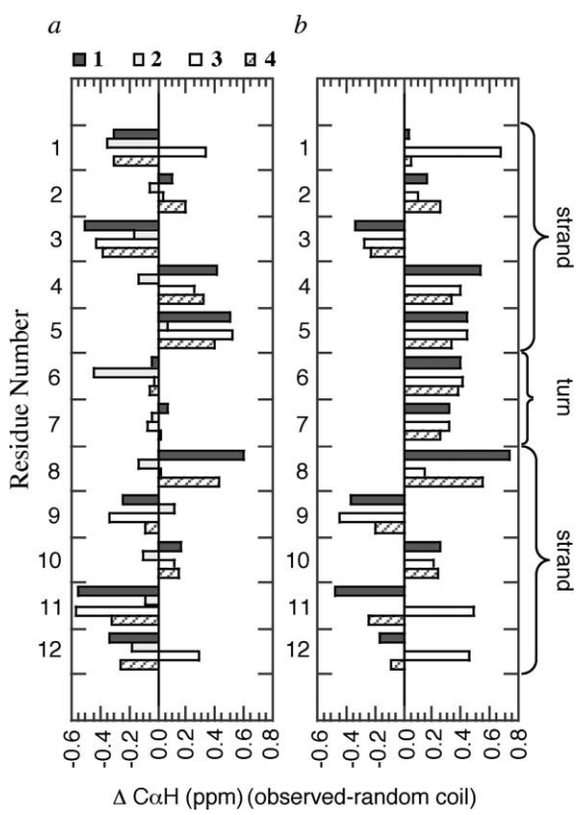

Fig. 4 Chemical shift deviations observed in the ^{1}H NMR spectra of **1**–**4** as compared with (a) random coil values taken from ref. 89 and (b) the chemical shift values observed in **2**.

Simulated annealing molecular dynamics analysis was done by using the NOE-derived distance restraints. All the sampled conformations for **1** were part of a single class with little deviation observed in the backbone dihedrals between the conformations. An overlay of the ten lowest energy conformations for **1** is shown in Fig. 5. The β-turn and Trp–zip interactions are also similar in all ten structures, whereas the C- and N-terminal residues adopt the widest variety of conformations in both the backbone and side chains. The average RMSD (root mean

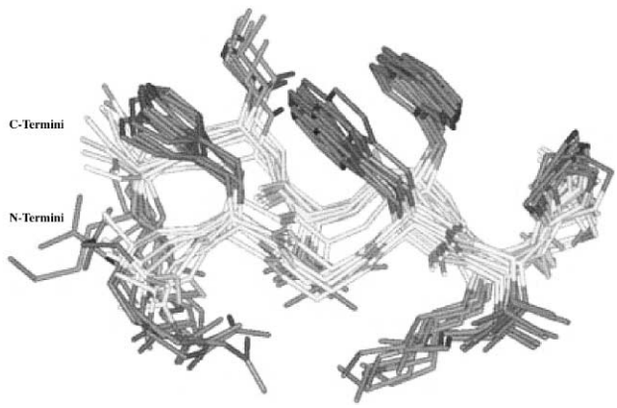

Fig. 5 An overlay of the ten lowest energy structures of **1** from the simulated annealing molecular dynamics calculations. The backbone atoms are shaded lighter than the side chains and hydrogen atoms are omitted for clarity.

square deviation) between the backbone atoms of these conformers is 0.49 ± 0.15 Å. This modeling result is consistent with the observed experimental data and our interpretation of the splaying of the β-hairpin ends. It is also important to note that side chain conformations were not constrained to any degree but were still observed to be very similar in all of the resulting low energy structures for **1**.

In contrast, simulated annealing molecular dynamic calculations employing NOE-derived distance constraints for **3** produced a series of conformers including some that were significantly different from one another. The average RMSD between the ten lowest energy structures is more than 1 Å. An overlay of the ten lowest energy conformations for **3** is shown in Fig. 6. Seemingly the cyclization constrains the peptide backbone and allows the side chains to adopt multiple conformations of approximately equal energy. This is consistent with the reduction in the 227 nm CD signal that suggests the Trp–zip interaction is different in **3** as compared with **1**.

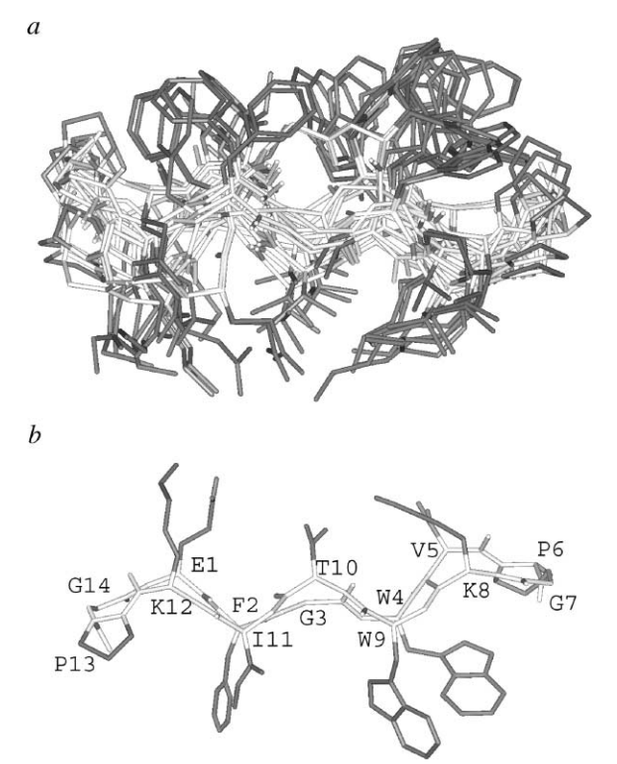

Fig. 6 (a) An overlay of the ten lowest energy structures of **3** from the simulated annealing molecular dynamics calculations and (b) the mean conformer. The backbone atoms are shaded lighter than the side chains and hydrogen atoms are omitted for clarity.

Peptide **5** was designed as a model containing a PheGly dipeptide sequence with similar cross strand interactions as compared with **1**, albeit with both the Phe and Gly in an alternate N-terminal strand position of the β-hairpin hydrogen bond register (non-hydrogen bonded *vs.* hydrogen bonded) as compared with **1**. Instead of pairing Phe with Ile as in **1**, a second cross strand aromatic interaction between Phe and Tyr was chosen for **5**. It is noteworthy that the Trp–zip motif was moved closer to the ends of the two β-strands. It is now known that an aromatic cluster is more stabilizing closer to the β-turn of the β-hairpin motif,[37] although this location was chosen in anticipation of stabilizing the ends of the two strands in the β-hairpin. The resulting design was expected to put the two aromatic clusters on opposite sides of the β-sheet structure and perhaps prevent the diagonal interactions hypothesized to contribute to differences in the side chain interactions between **1** and **3**. In addition, we exchanged the Val residue in **1** with a β-branched Ile, since the later residue and its structurally distinct side chain introduced the possibility of producing more information in the ^{1}H NMR analysis. These changes were anticipated to retain stabilization of β-hairpin formation in water, reduce the significance of diagonal interactions, and provide a peptide with a Gly β-strand residue in a non-hydrogen bonding location of a β-strand.

Peptide **6** replaces Gly4 in **5** with a Ser in order to examine the role of the Gly β-strand residue. In **7** the W2–W11 cross strand pair is exchanged with the G4–T9 cross strand pair, effectively placing the Trp–zip interaction in the same location within the β-hairpin as it is found in **1**. This exchange examines the conformation when the aromatic residues are still next to one another within a β-strand and a Gly is still in a non-hydrogen bonding location of the β-strand.

Fig. 7 compares the CD spectra of **5**–**7** with **1** in water. The CD signals for **5** and **6** are similar to one another but yet clearly different than the signal for either **1** or **7**. In **5** and **6** the Trp–zip exciton coupling is stronger at 227 nm as compared to **1**, while still weaker at 215 nm as compared to **1**. Another difference between these peptides is the observed maximum near 200 nm for **5** and **6** *vs.* about 194 nm for **1** and **7**. In contrast, the spectrum for **7** is closer to **1** in terms of the observed minima and maximum locations, if not in the absolute intensities.

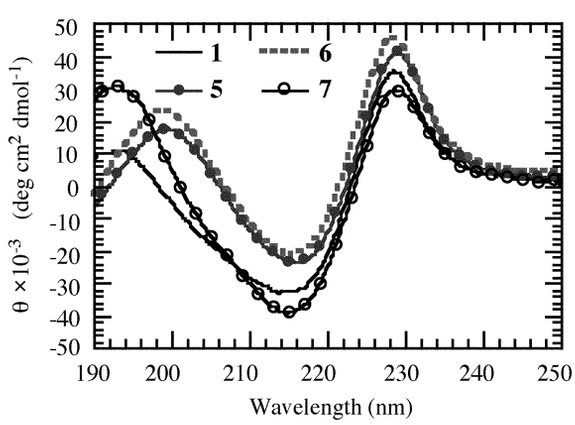

Fig. 7 The CD spectra of **5**–**7** recorded in water and compared to **1**.

The chemical shift assignments, excluding those for the aromatic ring hydrogens, are given in Table 3 for **5** and **7**. Also included in Table 3 are the $C_\alpha H$ chemical shift deviations from published random coil values.[89]

The observation of $d_{(NN)}$ NOEs in **5** between amino acid residue pairs G7–K8 and I5–K8 supports the formation of turn conformation centered around the region I5–K8. Several other NOEs are also observed, although most are inconsistent with the expected β-hairpin conformation having the correct hydrogen bond register. In particular, the backbone $d_{(NN)}$ NOE between W2 and W11 is observed. These two residues are in

Table 3 Chemical shifts (ppm), coupling constants and chemical shift deviations (ppm) for **5** and **7**[a]

	Residue	NH	$C^{\alpha}H$	$^{3}J_{\alpha NH}$/Hz	$C^{\beta}H$	$C^{\gamma}H$	$C^{\delta}H$	$C^{\varepsilon}H$	NH_3^+	$\Delta\delta C^{\alpha}H$	$\Delta\delta NH$
5:	Glu1		3.42		1.71, 1.82	1.91, 2.10				−0.87	
7:			4.20		2.18	2.38, 2.42				−0.09	
	Trp2	9.47	4.79	9.0	2.52, 2.95					0.12	1.01
	Gly2	8.58	3.27, 3.99							−0.02	−0.08
	Phe3	8.79	4.86	8.5	2.26, 2.83					0.24	0.18
		7.36	4.40	Overlap	2.86, 3.14					−0.22	−1.25
	Gly4	8.55	3.82							−0.19	−0.11
	Trp4	8.63	5.21	Overlap	3.10, 3.45					0.54	0.17
	Ile5	8.47	4.73	8.5	1.93	1.21, 1.53	0.84, 0.96			0.55	0.05
	Val5	9.48	4.68	9.0	2.08	0.99, 1.04				0.55	0.97
	D-Pro6		4.39		2.34	2.00, 2.06	3.82			−0.05	
			4.43		2.00, 2.10	2.20, 2.38	3.82, 3.97			−0.01	
	Gly7	8.88	3.90, 3.99							−0.02	0.22
		8.72	3.97							−0.04	0.06
	Lys8	7.90	4.63	9.0	1.83	1.38, 1.48	1.71	2.98	7.14, 7.58	0.31	−0.77
		8.23	4.88	9.5	1.90	1.41, 1.51	1.75	3.03		0.56	−0.44
	Thr9	8.06	5.14	8.5	3.96					0.75	−0.46
	Trp9	8.63	4.27	Overlap	1.88, 2.69					−0.40	0.17
	Tyr10	8.73	5.32	8.0	3.12					0.76	0.14
	Ile10	8.45	3.99	8.5	1.01	0.58				−0.19	−0.07
	Trp11	9.20	5.05	9.0	2.52, 3.04					0.38	0.74
	Thr11	7.79	4.20	8.5	4.05	1.14				−0.19	−0.73
	Tys12	7.97	4.09	8.0	1.62	1.19	1.36	2.60	7.10, 7.32	−0.23	−0.70
		7.95	4.14	7.5	1.77	1.32	1.64	2.90		−0.18	−0.72

[a] Peptides **5** and **7** are organized as lines 1 and 2, respectively, for any given row in this table. Amino acid mutations are specifically indicated under the residue column. Random coil values were taken from ref. 89.

non-hydrogen bonding positions and were expected to point their backbone NH groups away from one another and toward the solvent. Surprisingly, NOEs between I5:δHs with W11:4H and W11:5H are also observed. These are inconsistent with a β-hairpin conformation given the expected distance between these residues. It is more likely that these NOEs arise from a separate population of molecules that are largely unfolded, partially folded, alternately folded or combinations thereof. For this reason we did not add these NOEs to the restraint file for constrained molecular dynamic simulations. The NOE contacts for **5** that were used for molecular dynamics are summarized graphically in the supporting information. †

We prepared the Ser analog, **6**, as a test of whether the unusual and unexpected NOEs between W2 and Y10 may have been influenced by the flexibility of the Gly4 residue. However, mutating the Gly residue to a Ser resulted in a similar CD spectrum as compared to **5** (Fig. 7). Therefore, a detailed ^{1}H NMR study was not done, expecting that the peptide conformation was to be the same for **6** as in **5**. This comparison suggests that the unusual conformation of **5** is not a result of the Gly4 flexibility.

We then turned our attention to **7** which exchanges the W2–W11 and G4–T9 cross strand pair positions from **5**, yielding a peptide with the Trp–zip interaction closer to the β-turn but still with adjacent aromatic residues within each β-strand. Based on the similar CD spectra for **5** and **6**, it was anticipated that the backbone torsion angle(s) that allowed the hydrophobic groups to cluster together in **5** must be altered at one or more of the aromatic residues. Thus, it was expected that moving the Trp residues closer to the β-turn would still test whether a similar hydrophobic cluster could form in **7** and thereby alter the peptide conformation. Of greater concern to us about this design was whether the twist of the β-sheet factored into the orientation of the strand residues or whether the first cross strand pair of the cluster needed to be in a non-hydrogen bonded position or both. Thus, in order to further promote the hydrophobic cluster observed in **5**, we decided to change the Tyr back to an Ile in order to increase favorable dispersion forces—an expectation based on the results from the Wilcox torsional balance.[93] It may have been more favorable in hindsight to retain the aromatic interaction, as these associations have been shown within the context of a β-hairpin to be more favorable thermodynamically than purely hydrophobic interactions.[94]

The CD spectrum of **7** more closely parallels the spectrum observed for **1** rather than that for **5** or **6** (Fig. 7). Thus, it was not surprising that the NOE contacts observed for **7** are consistent with a regular β-hairpin structure.

The NOE contacts for **7** are summarized graphically in the supporting information. † Interestingly, NOE contacts between G2 and T11 were also observed and suggest that the ends the two β-strands in **7** are more ordered than those of **1**. This is consistent with the increased intensities at 215 and 200 nm in the CD spectrum of **7** as compared with **1**. The similarity in structure between **1** and **7** *vs.* that found in **5** is also evident when the chemical shift deviations are compared side-by-side (Fig. 8). In each peptide there are residues that deviate from the expected downfield chemical shifts common for the β-strand conformation; yet, the observed values are more similar between **1** and **7** than with those of **5**.

The NOE contacts for **5** were used to calculate a series of solution structures by employing simulated annealing molecular dynamics calculations. Aside from NOEs that define the β-turn and the cross strand contacts surrounding the β-turn

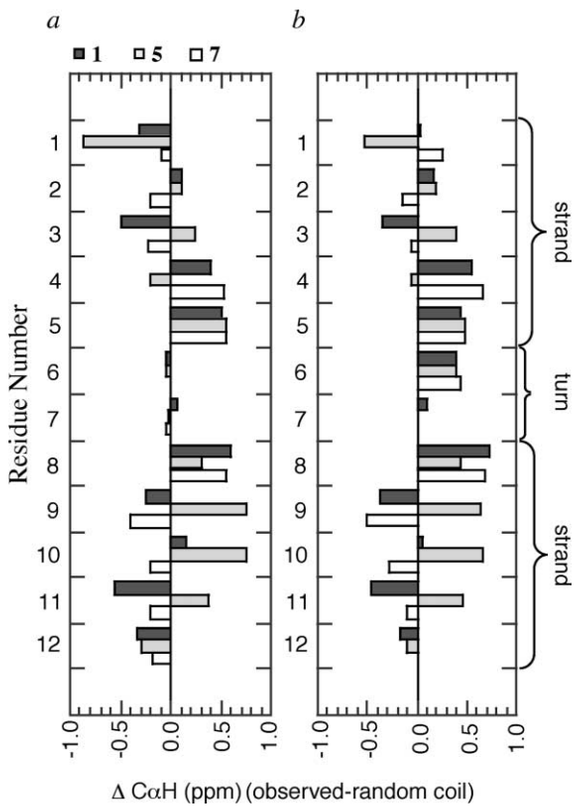

Fig. 8 Chemical shift deviations observed in the ^{1}H NMR spectra of **1**, **5** and **7** as compared with (a) random coil values taken from ref. 89 and (b) the chemical shift values observed in **2**.

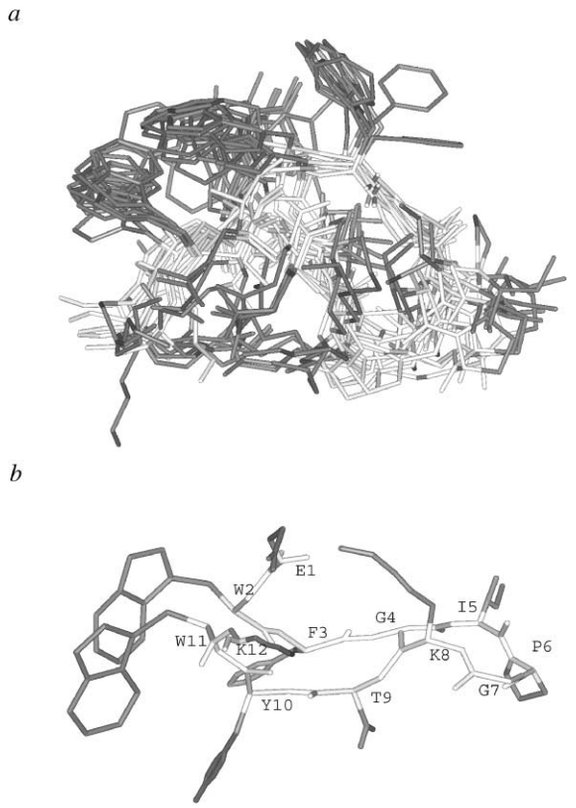

Fig. 9 (a) An overlay of the ten lowest energy structures of **5** from the simulated annealing molecular dynamics calculations and (b) the mean conformer. The backbone atoms are shaded lighter than the side chains and hydrogen atoms are omitted for clarity.

region, a strong W2–W11 $d_{(NN)}$ NOE, a W2–W11 side chain NOE and a W2–Y10:αH NOE were included in these calculations. As expected and consistent with these NOEs, the conformations found in this analysis contain a twisted β-strand that result in all four aromatic rings in close proximity and on the same face of the β-sheet. An overlay of the ten lowest energy conformations for **5** from this analysis is shown in Fig. 9.

In contrast to **5**, the NOEs for **7** were consistent with formation of a β-hairpin conformation. The observed NOEs were used in simulated annealing molecular dynamics calculations. An overlay of the ten lowest energy conformations for **7** from this analysis is shown in Fig. 10.

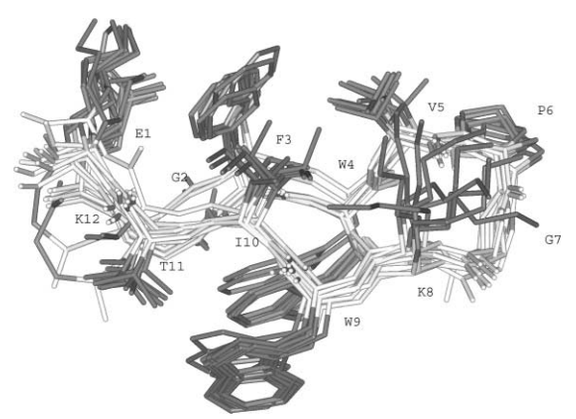

Fig. 10 An overlay of the ten lowest energy structures of **7** from the simulated annealing molecular dynamics calculations. The backbone atoms are shaded lighter than the side chains and hydrogen atoms are omitted for clarity.

Discussion

Peptide 1 adopts a β-hairpin conformation in water

Significant advances in both β-hairpin design and characterization have been made in the past few years with many important criteria for β-hairpin formation and stabilization now being determined in systematic fashion. Indeed, the design of **1** includes the well known type II′ β-turn sequence D-ProGly,[19–25] cross strand aromatic interactions between two Trp residues (Trp–zip interaction),[38] as well as a N- and C-terminal Glu–Lys cross strand electrostatic interaction [30] —all features previously studied within β-hairpins and shown to favor their formation.

Peptide **1** undergoes an increase in secondary structure upon addition of MeOH as determined by CD analysis; however, the increase in signal from that recorded in water with that found in 50% MeOH is small (<20%). Also, no significant differences are observed when comparing the CD signal observed at pH 4 with that recorded at pH 7. The NOEs observed for **1** in water are also consistent with a folded β-hairpin and support the conclusion that this is a predominant conformation in water. A 10-fold dilution of the NMR sample led to no differences in either the chemical shift values or the signal widths, providing support that **1** is also monomeric under the conditions of the NMR experiments. We therefore conclude that **1** is a β-hairpin in water at pH 7. Regardless of our expectation that the design features would yield a β-hairpin, it was still satisfying to determine that **1** is both folded and stable in this conformation in water.

Unfolded and folded models of 1 yield ambiguous results

Mutating the D-Pro residue to L-Pro precludes the formation of the D-ProGly type II β-turn and is thereby used to generate an unfolded peptide control for spectroscopic comparison.[78] On the other hand, incorporation of a second D-ProGly type II β-turn yields a cyclic peptide to serve as a folded control for spectroscopic comparison.[78] A major advantage in the use of these variants as unfolded and folded models over other methods of peptide conformational analysis is that the context of each amino acid within the sequence remains similar.

Indeed, amino acid context has been shown to influence both $C_\alpha H$ chemical shifts[52] and even the β-sheet propensities of amino acids.[16] Another important method of conformational analysis has been to compare the NMR chemical shift differences between residues recorded within a glycine random coil pentapeptide and corrected for sequence-dependency with the observed values.[89] These chemical shift differences have been shown to correlate with types of secondary structure like α-helices or β-sheets, thereby providing additional support for a particular fold.

Conformational analysis of **2** and **3** by NMR spectroscopy was expected to yield data providing the percentage of folded β-hairpin and the thermodynamic stability for **1**. We expected that the CD data could be referenced to our estimate of folded conformation from the NMR data, and that CD would then represent a faster method for determining the relative influence of solvent, pH, and temperature on the conformation. Comparison of the CD signals for **1**–**3** in Fig. 3 show that **2** is indeed a random coil with little comparative signal strength and that the CD signal for **3** is similar to **1**. However, a surprising difference between **1** and **3** was the Trp–zip exciton coupling signal at 227 nm which was smaller in **3** than in **1**. Both **1** and **3** had a similar signal intensity at 215 nm and we think this is evidence of **3**—having been constrained by the cyclization—as being less dependent on cross strand or diagonal interactions to stabilize the β-hairpin. Thus, **3** folds as a model β-hairpin but contains a different aromatic cluster wherein the Trp–zip interaction has a less intense CD signal. The reduction in exciton signal at 227 nm can be expected to yield some reduction in signal strength at 215 nm. Thus, the similar signal strength at 215 nm between **1** and **3** is taken as evidence that **1** is not a fully folded (*i.e.*, 100%) β-hairpin. A recent molecular modeling study of a Trp–zip β-hairpin suggests that the folding process of this peptide does not contain a dominant pathway, but instead has multiple folding transitions.[70] It therefore seems reasonable that the end-state of the folding process may also contain variable aromatic cross-strand interactions between the side chains.

The NMR experiments on **2** and **3** support, in part, the above conclusions. There was very little chemical shift dispersion in **2**, supporting the formation of a random coil conformation. In contrast, both **1** and **3** have significant chemical shift dispersion and even display splitting for the two $C_\alpha H$ protons in the β-strand Gly residue, evidence that the peptides are in folded conformations. Unfortunately, the chemical shift deviations of **1** and **3** as compared with published random coil values (Fig. 4) do not show a consistent trend that can be interpreted in terms of particular secondary structure formation. It is noteworthy that the chemical shifts for **2** also deviate from the published random coil values. Conformational analysis using the $C_\alpha H$ NMR chemical shift data for **2** as the standard would suggest that **1** forms very little β-hairpin structure (percentages being residue dependent). On the other hand, comparison of **2** against random coil values suggests that this peptide is folded (percentages being residue dependent), inconsistent with the method of analysis.[78] This reinforces the idea that the local sequence influences the observed chemical shift value as well as suggesting that neither the unfolded model peptide nor the model random coil values can accurately predict the conformation for this peptide.

We originally planned to use NMR data to quantify the folding of **1**, followed by the thermodynamic analysis of analogs containing β-strand peptidomimetics. Unfortunately the variations in the data between **1** and the unfolded (**2**) and folded models (**3**) have precluded a meaningful analysis. For this reason quantification of the folding has not been included in this paper. It may be possible to use the data in the future for such an analysis—provided a deeper understanding of the local effects or other parameters influencing these data become better known.

Mutational analysis of 1

To help begin unraveling these parameters, we have prepared mutants of **1** that explore the role of our design features in both the folding and spectroscopic characteristics of **1**. The Trp–zip feature was removed from **4** and replaced with an aromatic cluster. This leads to significant differences in the CD spectrum of **4** as compared with **1** and **3**, even though **4** was determined to be partially folded in a conformation with interactions between these aromatic side chains. Indeed, many of the NMR features observed for **1** or **3** or both are also present in the spectra for **4**, including β-turn NOEs and significant splitting of the β-strand Gly $C_\alpha H$s.

Peptides **5**–**7** contain a similar set of amino acids found in **1**–**4**, although the sequence of the β-strand residues was altered. The most significant difference was that the aromatic side chains were moved from locations that would place them on either top or bottom of a β-hairpin conformation in **1**, **3** or **4** to placing them on top and bottom of a β-hairpin conformation in **5**–**7**. The β-strand Gly residue in **1** is located in a non-hydrogen bonding site in **5**. This peptide has a significantly different CD spectrum as compared with **1** (Fig. 7). Moreover, long-range NOEs for **5** were identified between the aromatic side chains designed to be on opposite sides (top and bottom) of the β-hairpin conformation. Simulated annealing molecular dynamic calculations identified a family of conformations that contain a twisted β-strand with all of the aromatic side chains on the same side of the peptide, allowing them to interact with one another. Replacing the β-strand Gly residue in **5** with a Ser yields **6**, a peptide that gives a similar CD spectrum to **5**.

Peptide **7** contains aromatic/hydrophobic residues in adjacent β-strand positions and was created by transposition of the 2/3 residue pair and 10/11 residue pair, respectively, in **1**. This peptide retains the Trp–zip in the same non-hydrogen bonding site as in **1**. Although **7** does not contain the cross strand Phe and Tyr present in **4**, we anticipated the Ile cross strand, lateral, and diagonal interactions with the aromatic rings would be as favorable. Thus, if lateral or diagonal interactions or both were responsible, even in part, for the unusual conformation found in **5** and anticipated for **6**, then peptide **7** was also expected to favor this unusual conformation.

The CD spectrum of **7** compares better with **1** than with **5** or **6** (Fig. 7), the most significant differences between **1** and **7** have to do with the absolute intensities of the signal. In order to help us better compare the peptides in terms of their CD spectrum, we compared the ratio of intensities observed at 227 nm relative to 215 nm (Fig. 11). These ratios vary considerably over the different peptides, from ratios as measured in water of 0.3 in **2**

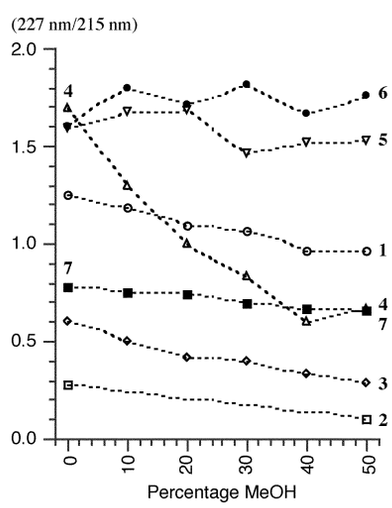

Fig. 11 Illustration comparing the ratio of CD intensity between 227 and 215 nm with the percentage of MeOH. This ratio varies across the peptides although it appears that **4** undergoes the most significant folding upon addition of MeOH.

to 1.7 in **4**. This was expected since the factors contributing to the signals at these wavelengths were different between the peptides (*e.g.*, Trp–zip interaction is missing in **4**). It was interesting, however, to follow this ratio as a function of MeOH concentration. Only the ratio for **4** varies significantly over the concentration change, while peptides **1**–**3** and **7** decrease only slightly with increasing percentages of MeOH (resulting from a greater contribution from the signal at 215 nm). This is consistent with increasing folded conformation of the peptide β-strands upon MeOH addition and the role of alcohol cosolvents in promoting hydrogen bonding.[95] Our interpretation of this data is that **4** is less folded than **1** in water and benefits significantly from the presence of MeOH, whereas **2** remains unfolded even in the presence of MeOH. The trend for **5** and **6** appears different as compared with the other peptides (even the unfolded model, **2**). These differences are in part due to the greater contribution by the aromatic CD signals in **5** and **6** but also in the fact that the ratio does not change systematically with MeOH addition. This supports our conclusion that the formation of an aromatic cluster drives the unusual conformation observed for **5** and would be expected in **6** by comparison of their CD spectra.

Temperature is an important factor in assessing the folding thermodynamics of peptides by their $C_\alpha H$ chemical shifts.[96] Fig. 12 compares the temperature-dependence for the chemical shift of the C_αHs for **1** and **5**. Neither peptide contains $C_\alpha H$ chemical shifts that deviate significantly as a function of temperature, consistent with the NMR and CD data that suggests these two peptides have folded conformations in water that undergo little change upon addition of MeOH. On the other hand, there are several interesting features to note about this chemical shift data. For example, both **1** and **5** have splitting in the β-turn Gly (G7) and this splitting does not vary across the observed temperatures. In **1**, the β-strand Gly (G3) is also split and does not change as a function of temperature, while there is no splitting observed for the β-strand Gly (G4) in **5**. The F2 and I11 $C_\alpha H$ chemical shifts also move downfield slightly in **1**, against the general trend for residues 3–10 and a result consistent with our interpretation of enhanced folding of the ends of

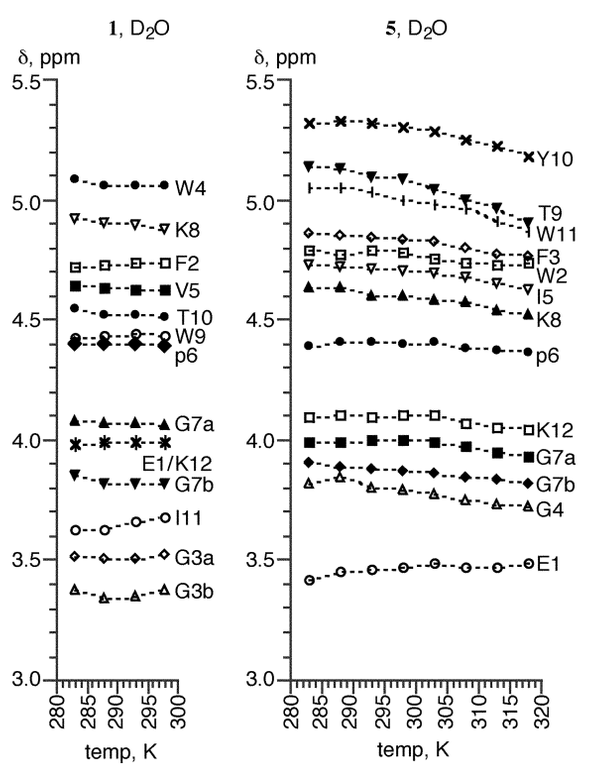

Fig. 12 Temperature-dependence of the chemical shift (ppm) for the $C_\alpha H$ protons of **1** and **5** as recorded in D_2O at pH 5.0. The dashed lines between measured data are intended only to guide the eye.

Table 4 The average backbone torsion angles and the RMSDs as determined in the ten lowest energy structures of **1**, **3**, **5** and **7**, respectively

		Peptide			
Residue	∠	**1**	**3**	**5**	**7**
2	ϕ	−116 ± 20	−125 ± 21	74 ± 5	**−69 ± 85**
	ψ	117 ± 17	109 ± 15	**2 ± 92**	**88 ± 88**
3	ϕ	−85 ± 3	**−45 ± 120**	**−66 ± 98**	−135 ± 6
	ψ	86 ± 5	**46 ± 104**	**57 ± 96**	130 ± 3
4	ϕ	−101 ± 3	−88 ± 13	**−61 ± 157**	−108 ± 4
	ψ	102 ± 8	113 ± 6	**−31 ± 108**	101 ± 4
5	ϕ	−136 ± 6	−123 ± 6	−136 ± 19	−95 ± 8
	ψ	77 ± 3	87 ± 6	104 ± 15	106 ± 2
6	ϕ	59 ± 7	75 ± 2	70 ± 4	67 ± 11
	ψ	−109 ± 5	**−84 ± 54**	**−60 ± 68**	**−43 ± 73**
7	ϕ	−61 ± 6	**−85 ± 62**	**−22 ± 91**	**−56 ± 110**
	ψ	−34 ± 6	18 ± 49	−33 ± 48	56 ± 30
8	ϕ	−81 ± 5	−133 ± 40	−100 ± 31	−141 ± 23
	ψ	103 ± 9	120 ± 15	95 ± 42	135 ± 8
9	ϕ	−124 ± 7	−100 ± 16	−124 ± 26	−81 ± 5
	ψ	86 ± 5	107 ± 9	**59 ± 103**	109 ± 5
10	ϕ	−93 ± 4	−100 ± 16	**30 ± 68**	−132 ± 12
	ψ	95 ± 6	107 ± 9	133 ± 18	115 ± 10
11	ϕ	−86 ± 9	−111 ± 26	−43 ± 33	−107 ± 17
	ψ	116 ± 10	102 ± 15	**105 ± 63**	132 ± 13

Emboldened torsion angles are those that have observed deviations greater than 50° over the ten lowest energy conformations.

the β-strands upon MeOH addition. In this case, the increased temperature could further drive hydrophobic interactions between the Ile and the aromatic side chains, further rigidifying the ends of the β-hairpin. The nearly linear appearance of the chemical shift deviations in Fig. 12 preclude the determination of thermodynamics from this data by plotting δ *vs.* T—a previously noted difficulty in a minimal β-hairpin peptide.[96]

Conformational flexibility in the β-strand and β-turn residues

The average backbone torsion angles for **1**, **3**, **5** and **7** and the root mean square deviation (RMSD) for the backbone residues resulting from an overlay of the ten lowest energy structures is shown in Table 4. Comparison of the results for **1** with those for **3**, **5** and **7** highlights both the flexibility that residues adopt at the β-strand ends as well as about the Gly residue of the β-turn in the later three peptides. Varied β-hairpin folding has been previously described when the location of the hydrophobic cluster is changed with respect to the β-turn residues.[33,37] This is certainly one component of the differences between **1** as compared with **5** and **7**. Selected β-strand residues in all four peptides are observed in disparate conformations as compared with those for an ideal anti-parallel β-sheet (ϕ = −140°, ψ = 135). These values are also different than one another for certain residues when comparing the same positions across different peptides. For example, residue 8 is different for peptide **1** as compared with **3**, **5** and **7**, although the larger standard deviations in the torsion angles of **3**, **5** and **7** for this residue do describe conformations that largely overlap one another. The conformational flexibility—particularly of **3** and **5**—is further illustrated by comparing the RMSD for the overlays of the ten lowest energy structures as given in Table 5.

The results as applied to β-hairpin thermodynamic analysis

The design features included in **1** proved reliable for the formation of a β-hairpin conformation as expected. However, use of either unfolded and folded model peptides or published random coil values in order to quantify the population of the folded conformation in **1** failed. Deviations such as those described herein have been attributed to factors such as the dynamics of the β-hairpin structure, the local residues influence on the $C_\alpha H$ chemical shifts, and the position of the residue

Table 5 Statistical analysis of the ten lowest energy structures from the 200 ps molecular dynamics analysis

Peptide	RMSD of conformers (Å)		
	Residues 2–11	Residues 4–9	Residues 5–8
1	0.49 ± 0.15	0.29 ± 0.09	0.16 ± 0.04
3	1.69 ± 0.71	1.02 ± 0.40	0.55 ± 0.37
5	1.58 ± 0.78	1.39 ± 0.83	0.56 ± 0.40
7	0.53 ± 0.18	0.37 ± 0.26	0.37 ± 0.33

in the β-hairpin (hydrogen bonded or non-hydrogen bonded residue as well as location with respect to the β-turn).[9]

Thermodynamic analysis of β-hairpin folding begins with the general assumption of a two-state phenomenon (unfolded Δ folded). We have not observed evidence for any cooperativity between the β-turn formation and the hydrophobic cluster formation—a phenomenon previously observed for similar peptides and favoring the validity of the two-state approach.[37] In contrast, there is evidence in our data for partial folding wherein the β-strands are dynamic but the β-turn and hydrophobic interaction are largely intact. This multi-state folding model has also proposed recently on the basis of $C_\alpha H$ chemical shift data for similar peptides in response to temperature.[96]

The results as applied to dissecting folding or peptidomimetic influences

Mutational analysis of proteins is widely used to dissect interactions significant to the folding and thermodynamic stability of the protein. This approach has even been used to explore the thermodynamic contribution of a hydrogen bond in a protein structure.[97–100] In similar fashion, a thioamide has been incorporated into a β-hairpin in order to observe the structural change on the peptide folding.[101] These are complementary methods for determining the consequences of a structural change. The proteins are generally able to accommodate the changes and thereby yield some useful comparison with the native structure. Yet, there are so many favorable interactions in a protein that compensating interactions may mask the effects resulting from a change in structure. There are fewer stabilizing interactions in a peptide and so changes to the structure may lead simply to a random coil—providing only a qualitative comparison with the parent peptide. Unfortunately, the variations in the β-hairpins described in this work also preclude using these structures for anything more than qualitative comparison following some structural change. It may be that small protein domains offer the best compromise and recently peptidomimetic β-turns have been incorporated into the WW motif for subsequent thermodynamic comparisons.[102]

Conclusion

This work illustrates the combined use of favorable design elements to yield a folded β-hairpin, **1**, that contains an unfavorable Gly in a hydrogen bonded location of a β-strand. The use of accepted NMR methods for quantification of the folding in **1** fails with this peptide. Our data suggests that the cyclic model peptide, **3**, adopts different side chain interactions that interfere with the quantification method. An alternative model peptide with a Gly in a non-hydrogen bonded location, **5**, resulted in NMR data that supports a very unusual conformation of the peptide backbone. This did not appear to be the result of the Gly residue or the alternate design strategy that attempted to create a hydrophobic cluster on both the top and bottom of the β-hairpin. It is possible that the location of the hydrophobic cluster in the β-hairpin (further from the β-turn) was significant in the folding of **5**, although no peptides have yet been prepared to test this hypothesis.

Acknowledgements

The authors thank the KSU biotechnology center for HPLC and MALDI MS access and Ralf Warmuth for access to the CD spectrophotometer. This work was supported in part by a NIH–COBRE award 1-P20-RR15563 and matching support from the state of Kansas.

References

1 E. de Alba, M. A. Jimenez, M. Rico and J. L. Nieto, *Fold. Des.*, 1996, **1**, 133–144.
2 K. Gunasekaran, C. Ramakrishnana and P. Balaram, *Protein Eng.*, 1997, **10**, 1131–1141.
3 C. K. Smith and L. Regan, *Acc. Chem. Res.*, 1997, **30**, 153–161.
4 S. H. Gellman, *Curr. Opin. Chem. Biol.*, 1998, **2**, 717–725.
5 F. Blanco, M. Ramírez-Alvarado and L. Serrano, *Curr. Opin. Struct. Biol.*, 1998, **8**, 107–111.
6 M. Ramírez-Alvarado, T. Kortemme, F. J. Blanco and L. Serrano, *Biorg. Med. Chem.*, 1999, **7**, 93–103.
7 E. Lacroix, T. Kortemme, M. Lopez de la Paz and L. Serrano, *Curr. Opin. Struct. Biol.*, 1999, **9**, 487–493.
8 J. Venkatraman, S. C. Shankaramma and P. Balaram, *Chem. Rev.*, 2001, **101**, 3131–3152.
9 M. S. Searle, *J. Chem. Soc., Perkin Trans. 2*, 2001, 1011–1020.
10 J. P. Schneider and J. W. Kelly, *Chem. Rev.*, 1995, **95**, 2169–2187.
11 C. L. Nesloney and J. W. Kelly, *Bioorg. Med. Chem.*, 1996, **4**, 739–766.
12 J. S. Nowick, E. M. Smith and M. Pairish, *Chem. Soc. Rev.*, 1996, **25**, 401–415.
13 J. S. Nowick, *Acc. Chem. Res.*, 1999, **32**, 287–296.
14 J. S. Nowick and J. O. Brower, *J. Am. Chem. Soc.*, 2003, **125**, 876–877.
15 M. B. Swindells, M. W. MacArthur and J. M. Thornton, *Nat. Struct. Biol.*, 1995, **2**, 596–603.
16 S. R. Griffiths-Jones, G. J. Sharman, A. J. Maynard and M. S. Searle, *J. Mol. Biol.*, 1998, **284**, 1597–1609.
17 S. J. Russell, T. Blandl, N. J. Skelton and A. G. Cochran, *J. Am. Chem. Soc.*, 2003, **125**, 388–395.
18 J. S. Merkel and L. Regan, *Fold. Des.*, 1998, **3**, 449–455.
19 T. S. Haque and S. H. Gellman, *J. Am. Chem. Soc.*, 1997, **119**, 2303–2304.
20 H. E. Stanger and S. H. Gellman, *J. Am. Chem. Soc.*, 1998, **120**, 4236–4237.
21 E. de Alba, M. Rico and M. A. Jimenez, *Protein Sci.*, 1999, **8**, 2234–2244.
22 C. Das, G. A. Naganagowda, I. L. Karle and P. Balaram, *Biopolymers*, 2001, **58**, 335–346.
23 P. Y. Chen, B. G. Gopalacushina, C. C. Yang, S. I. Chan and P. A. Evans, *Protein Sci.*, 2001, **10**, 2063–2074.
24 P.-Y. Chen, C.-K. Lin, C.-T. Lee, H. Jan and S. I. Chan, *Protein Sci.*, 2001, **10**, 1794–1800.
25 C. M. Santiveri, J. Santoro, M. Rico and M. A. Jiménez, *Protein Sci.*, 2004, **13**, 1134–1147.
26 E. J. Milner-White and R. Poet, *Biochem. J.*, 1986, **240**, 289–292.
27 B. L. Sibanda, T. L. Blundell and J. M. Thornton, *J. Mol. Biol.*, 1989, **206**, 759–777.
28 A. P. Cootes, P. M. G. Curmi, R. Cunningham, C. Donnelly and A. E. Torda, *Proteins*, 1998, **32**, 175–189.
29 M. S. Searle, G. W. Platt, R. Bofill, S. A. Simpson and B. Ciani, *Angew. Chem., Int. Ed.*, 2004, **43**, 1991–1994.
30 M. Ramirez-Alvarado, F. J. Blanco and L. Serrano, *Protein Sci.*, 2001, **10**, 1381–1392.
31 M. S. Searle, *Biopolymers*, 2004, **26**, 185–195.
32 S. J. Russell and A. G. Cochran, *J. Am. Chem. Soc.*, 2000, **122**, 12600–12601.
33 C. M. Santiveri, M. Rico and M. A. Jimenez, *Protein Sci.*, 2000, **9**, 2151–2160.
34 F. A. Syud, H. E. Stanger and S. H. Gellman, *J. Am. Chem. Soc.*, 2001, **123**, 8667–8677.
35 C. D. Tatko and M. L. Waters, *Protein Sci.*, 2003, **12**, 2443–2452.
36 C. D. Tatko and M. L. Waters, *J. Am. Chem. Soc.*, 2004, **126**, 2028–2034.
37 J. F. Espinosa, V. Muñoz and S. H. Gellman, *J. Mol. Biol.*, 2001, **306**, 397–402.
38 A. G. Cochran, N. J. Skelton and M. A. Starovasnik, *Proc. Natl. Acad. Sci. USA*, 2001, **98**, 5578–5583.
39 M. Favre, K. Moehle, L. Jiang, B. Pfeiffer and J. A. Robinson, *J. Am. Chem. Soc.*, 1999, **121**, 2679–2685.

40 H. E. Stanger, F. A. Syud, J. F. Espinosa, I. Giriat, T. Muir and S. H. Gellman, *Proc. Natl. Acad. Sci. USA*, 2001, **98**, 12015–12020.
41 S. Honda, N. Kobayashi and E. Munekata, *J. Mol. Biol.*, 2000, **295**, 269–278.
42 C. Guo, H. Levine and D. A. Kessler, *Proc. Natl. Acad. Sci. USA*, 2000, **97**, 10775–10779.
43 C. Guo, H. Levine and D. A. Kessler, *Phys. Rev. Lett.*, 2000, **84**, 3490–3493.
44 H. L. Schenck and S. H. Gellman, *J. Am. Chem. Soc.*, 1998, **120**, 4869–4870.
45 S. R. Griffiths-Jones and M. S. Searle, *J. Am. Chem. Soc.*, 2000, **122**, 8350–8356.
46 S. Ohnishi, A. Koide and S. Koide, *Protein Sci.*, 2000, **10**, 2083–2092.
47 R. Kaul, A. R. Angele, M. Jäger, E. T. Powers and J. W. Kelly, *J. Am. Chem. Soc.*, 2001, **123**, 5206–5212.
48 A. J. Maynard, G. J. Sharman and M. S. Searle, *J. Am. Chem. Soc.*, 1998, **120**, 1996–2007.
49 S. R. Griffiths-Jones, A. J. Maynard and M. S. Searle, *J. Mol. Biol.*, 1999, **292**, 1051–1069.
50 R. Zerella, P. Y. Chen, P. A. Evans, A. Raine and D. H. Williams, *Protein Sci.*, 2000, **9**, 2142–2150.
51 N. Carulla, C. Woodward and G. Barany, *Biochemistry*, 2000, **39**, 7927–7937.
52 G. J. Sharman, S. R. Griffiths-Jones, M. Jourdan and M. S. Searle, *J. Am. Chem. Soc.*, 2001, **123**, 12318–12324.
53 I. Nesmelova, A. Krushelnitsky, D. Idiyatullin, F. Blanco, M. Ramirez-Alvarado, V. A. Daragan, L. Serrano and K. H. Mayo, *Biochemistry*, 2001, **40**, 2844–2853.
54 R. Burgi, J. Pitera and W. F. van Gunsteren, *J. Biomol. NMR*, 2001, **19**, 305–320.
55 C. M. Santiveri, M. Rico and M. A. Jiménez, *J. Biomol. NMR*, 2001, **19**, 331–345.
56 C. M. Santiveri, J. Santoro, M. Rico and M. A. Jiménez, *J. Am. Chem. Soc.*, 2002, **124**, 14903–14909.
57 A. R. Dinner, T. Lazaridis and M. Karplus, *Proc. Natl. Acad. Sci. USA*, 1999, **96**, 9068–9073.
58 A. Kolinski, B. Ilkowski and J. Skolnick, *Biophys. J.*, 1999, **77**, 2942–2952.
59 H. Wang, J. Varady, L. Ng and S. S. Sung, *Proteins*, 1999, **37**, 325–333.
60 Z. Bryant, V. S. Pande and D. S. Rokhsar, *Biophys. J.*, 2000, **78**, 584–589.
61 A. M. Bonvin and W. F. van Gunsteren, *J. Mol. Biol.*, 2000, **296**, 255–268.
62 B. Ma and R. Nussinov, *J. Mol. Biol.*, 2000, **296**, 1091–1104.
63 P. Ferrara and A. Caflisch, *Proc. Natl. Acad. Sci. USA*, 2000, **97**, 10780–10785.
64 A. E. Garcia and K. Y. Sanbonmatsu, *Proteins*, 2001, **42**, 345–354.
65 J. Higo, N. Ito, M. Kuroda, S. Ono, N. Nakajima and H. Nakamura, *Protein Sci.*, 2001, **10**, 1160–1171.
66 J. Lee and S. Shin, *Biophys. J.*, 2001, **81**, 2507–2516.
67 B. Zagrovic, E. J. Sorin and V. Pande, *J. Mol. Biol.*, 2001, **313**, 151–169.
68 R. C. Reid, M. J. Kelso, M. J. Scanlon and D. P. Fairlie, *J. Am. Chem. Soc.*, 2002, **124**, 5673–5683.
69 X. Wu and B. R. Brooks, *Biophys. J.*, 2004, **86**, 1946–1958.
70 W. Y. Yang, J. W. Pitera, W. C. Swope and M. Gruebele, *J. Mol. Biol.*, 2004, **336**, 241–251.
71 A. B. Smith 3rd, S. D. Knight, P. A. Sprengeler and R. Hirschmann, *Bioorg. Med. Chem.*, 1996, **4**, 1021–1034.
72 J. L. Martin, J. Begun, A. Schindeler, W. A. Wickramasinghe, D. Alewood, P. F. Alewood, D. A. Bergman, R. I. Brinkworth, G. Abbenante, D. R. March, R. C. Reid and D. P. Fairlie, *Biochemistry*, 1999, **38**, 7978–7988.
73 N. Venkatesan and B. H. Kim, *Curr. Med. Chem.*, 2002, **9**, 2243–2270.
74 J. M. Ahn, N. A. Boyle, M. T. MacDonald and K. D. Janda, *Mini Rev. Med. Chem.*, 2002, **2**, 463–473.
75 V. J. Hruby and P. M. Balse, *Curr. Med. Chem.*, 2000, **7**, 945–970.
76 H. J. Dyson, M. Rance, R. A. Houghten, R. A. Lerner and P. E. Wright, *J. Mol. Biol.*, 1998, **201**, 161–200.
77 B. Imperiali, S. L. Fisher, R. A. Moats and T. J. Prins, *J. Am. Chem. Soc.*, 1992, **114**, 3182–3188.
78 F. A. Syud, J. F. Espinosa and S. H. Gellman, *J. Am. Chem. Soc.*, 1999, **121**, 11577–11578.
79 A. Trzeciak and W. Bannwarth, *Tetrahedron Lett.*, 1992, **33**, 4457–4560.
80 The calculated and observed molecular masses for the peptides are shown below. In each case the peptide was measured along with substance P as a standard, setting its $[M + H]^+$ peak to 1348.7.

Peptide	Formula	$[M + H]^+$ Calc.	$[M + H]^+$ Obs.
Substance P	$C_{63}H_{98}N_{18}O_{13}S$	1348.7	1348.7
1	$C_{72}H_{102}N_{16}O_{16}$	1448.7	1448.8
2	$C_{72}H_{102}N_{16}O_{16}$	1448.7	1448.7
3	$C_{79}H_{110}N_{18}O_{17}$	1584.9	1585.0
4	$C_{71}H_{103}N_{15}O_{16}$	1423.7	1424.3
5	$C_{76}H_{102}N_{16}O_{17}$	1512.8	1512.9
6	$C_{77}H_{104}N_{16}O_{18}$	1542.8	1542.6
7	$C_{72}H_{102}N_{16}O_{16}$	1448.7	1448.7

81 N. Sreerama, Venyaminov, S. Yu and R. W. Woody, *Anal. Biochem.*, 2001, **299**, 271–274.
82 N. Sreerama and R. W. Woody, *Anal. Biochem.*, 2000, **287**, 252–260.
83 N. Sreerama and R. W. Woody, *Anal. Biochem.*, 2000, **287**, 243–251.
84 R. W. Woody, *Methods Enzymol.*, 1995, **246**, 34–71.
85 F. J. Blanco, G. Rivas and L. Serrano, *Nat. Struct. Biol.*, 1994, **1**, 584–590.
86 N. Sreerama and R. W. Woody, *Protein Sci.*, 2003, **12**, 384–388.
87 E. H. Strickland, *CRC Crit. Rev. Biochem.*, 1974, **2**, 113–175.
88 I. B. Grishina and R. W. Woody, *Faraday Discuss.*, 1994, **99**, 245–262.
89 G. Merutka, H. J. Dyson and P. E. Wright, *J. Biomol. NMR*, 1995, **5**, 14–24.
90 Some of the $C_\alpha H$ signals for **3** were buried under the H_2O signal, and in order to determine NOE contacts between $C_\alpha H$ protons, a solution was prepared in D_2O.
91 D. S. Wishart, B. D. Sykes and F. M. Richards, *J. Mol. Biol.*, 1991, **222**, 311–333.
92 T. Blandl, A. G. Cochran and N. J. Skelton, *Protein Sci.*, 2003, **12**, 237–247.
93 E.-il Kim, S. Paliwal and C. S. Wilcox, *J. Am. Chem. Soc.*, 1998, **120**, 11192–11193.
94 C. D. Tatko and M. L. Waters, *J. Am. Chem. Soc.*, 2002, **124**, 9372–9373.
95 D. Roccatano, G. Colombo, M. Fioroni and A. E. Mark, *Proc. Natl. Acad. Sci. USA*, 2002, **99**, 12179–12184.
96 C. M. Santiveri, J. Santoro, M. Rico and M. A. Jimenez, *J. Am. Chem. Soc.*, 2002, **124**, 14903–14909.
97 E. Chapman, J. S. Thorson and P. G. Schultz, *J. Am. Chem. Soc.*, 1997, **119**, 7151–7152.
98 I. Shin, A. Y. Ting and P. G. Schultz, *J. Am. Chem. Soc.*, 1997, **119**, 12667–12668.
99 J. T. Koh, V. G. Cornish and P. G. Schultz, *Biochemistry*, 1997, **36**, 11314–11322.
100 W. Lu, M. A. Qasim, M. Laskowski Jr. and S. B. H. Kent, *Biochemistry*, 1997, **36**, 673–679.
101 J. H. Miwa, A. K. Patel, N. Vivatrat, S. M. Popek and A. M. Meyer, *Org. Lett.*, 2001, **3**, 3373–3375.
102 R. Kaul, A. R. Angeles, M. Jäger, E. T. Powers and J. W. Kelly, *J. Am. Chem. Soc.*, 2001, **123**, 5206–5212.